Journal of Photochemistry and Photobiology A: Chemistry 217 (2011) 10–21

Contents lists available at ScienceDirect

Journal of Photochemistry and Photobiology A: Chemistry

journal homepage: www.elsevier.com/locate/jphotochem

Meso-tetraphenyl porphyrin derivatives: The effect of structural modifications on binding to DMPC liposomes and albumin

Hanadi Ibrahim[a], Athena Kasselouri[a,*], Changjiang You[b,c], Philippe Maillard[d,e], Véronique Rosilio[b,c], Robert Pansu[f], Patrice Prognon[a]

[a] *Laboratoire de Chimie Analytique, EA4041, IFR 141, Univ Paris-Sud, 5 rue J-B. Clément, 92296 Châtenay-Malabry, France*
[b] *UMR 8612, Physico-Chimie des Surfaces, IFR 141, Univ Paris-Sud, 5 rue J-B. Clément, 92296 Châtenay-Malabry, France*
[c] *CNRS, UMR 8612, Univ Paris-Sud, 92296 Châtenay-Malabry, France*
[d] *Institut Curie, Centre de Recherche, Centre Universitaire, Univ Paris-Sud, F-91405 Orsay Cedex, France*
[e] *CNRS, UMR 176, Centre Universitaire, Univ Paris-Sud, F-91405 Orsay, France*
[f] *PPSM, UMR 8531 CNRS, École Normale Supérieure de Cachan, F-94235 Cachan cedex, France*

ARTICLE INFO

Article history:
Received 30 June 2010
Received in revised form 6 September 2010
Accepted 8 September 2010
Available online 17 September 2010

Keywords:
Glycoconjugated porphyrin
Aggregation
Lipophilicity
Albumin
DMPC liposome
Fluorescence

ABSTRACT

Three series of glycoconjugated and hydroxylated derivatives of 5,10,15,20-*meso*-tetraphenyl porphyrin (TPP) were studied in order to evaluate the effect of a porphyrin structure on its binding to dimyristoylphosphatidylcholine (DMPC) liposomes and to human serum albumin (HSA). The studied derivatives have been developed as potent photosensitizers for photodynamic therapy (PDT) of cancers. Steady state and time resolved fluorescence emission spectroscopy, Stern–Volmer quenching and fluorescence anisotropy were used for this evaluation. The lipophilicity of the compounds has been deduced from their retention time in reverse phase liquid chromatography. The results demonstrated that the more polar glycoconjugated compounds presented limited aggregation in aqueous media and very rapid binding kinetics to DMPC liposomes and HSA. Derivatives having intermediate or high hydrophobicity showed extensive auto-association in aqueous media and as a consequence slow association kinetics. The strength of porphyrin binding to DMPC liposomes also depended on their lipophilicity and was lower for the polar glycoconjugated analogues. The highest affinity for liposomes was observed for hydroxylated derivatives with intermediate lipophilicity. In contrast, the highest binding constant for albumin was observed for a polar tetra-glycoconjugated analogue. The depth of penetration into the phospholipid bilayer did not appear to be directly related to the global hydrophobicity of the compounds, but depended more on the number of apolar, non-substituted phenyl groups grafted to a tetrapyrrolic macrocycle. Furthermore, liposome–albumin competition studies revealed that the porphyrins were always mainly partitioned into the phospholipid bilayer.

1. Introduction

Porphyrins are a class of cyclic tetrapyrroles, which possess a highly conjugated, heterocyclic macrocycle. The presence of a 22-π electron system gives rise to their long wavelength absorption. As a result, porphyrins have attracted the attention of researchers for their application as photosensitizing agents (PS) in medicine and are of great interest in photodynamic therapy (PDT), a selective treatment against small superficial tumors or tumors accessible by endoscopy [1,2]. A key point of PDT is the uptake of the photosensitizing agent by tumor cells followed by their illumination with visible light. The photosensitization efficiency and intracellular localization of the PSs strongly depend on their structure, especially their hydrophobicity and the symmetry of distribution of polar and hydrophobic moieties around the macrocycle [3,4].

In the last decades, there has been an increasing interest in the synthesis and characterization of new porphyrin derivatives. In this context, many efforts have been focused by our groups on the development of neutral *meso*-tetraphenyl porphyrin (TPP) derivatives modified with glucose [5], galactose or mannose moieties [6] and more recently on the synthesis of photosensitizers bearing a glycodendrimeric moiety [7]. These modifications were developed in order to improve PS water solubility but also to favour the possibility of specific interactions with cellular membrane receptors as lectins [8].

Porphyrin interactions with biomolecules and membrane mimicking systems have been extensively studied. Hematoporphyrin [9–12], protoporphyrin [11] and their modified analogues [13,14], deuteroporphyrin [12,15], charged TPP derivatives [16] and *m*-

* Corresponding author. Tel.: +33 1 46835849; fax: +33 1 46835389.
E-mail address: athena.kasselouri@u-psud.fr (A. Kasselouri).

1010-6030/$ – see front matter © 2010 Elsevier B.V. All rights reserved.
doi:10.1016/j.jphotochem.2010.09.008

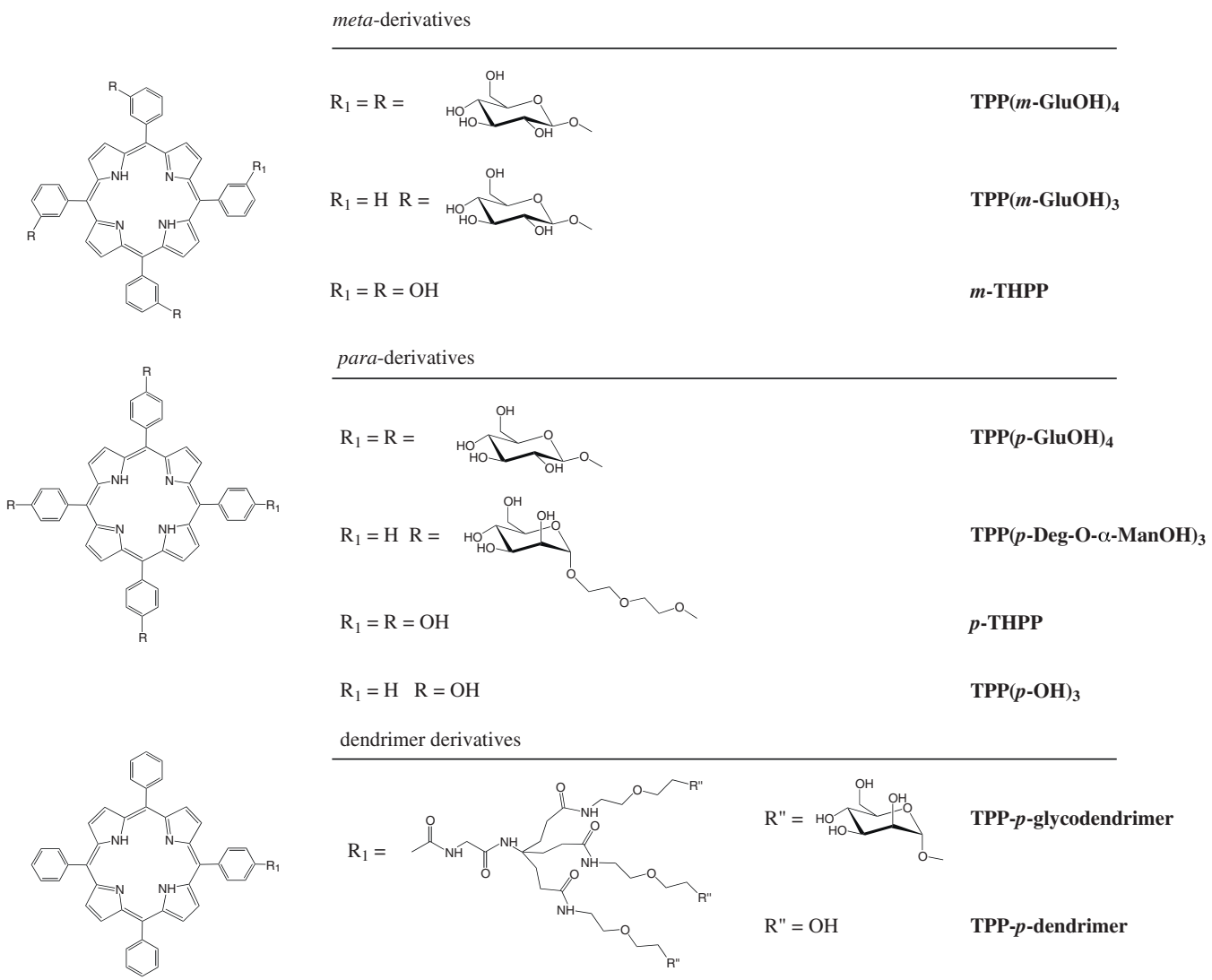

Fig. 1. Structure of tetra phenyl porphyrin (TPP) derivatives.

THPC (Foscan®) [17,18] received significant attention. Conversely, only few studies have been reported to this day on neutral TPP derivatives [19–21].

In the present work, we report on the evaluation of three series of tetraphenyl porphyrins (*meta*, *para* and dendrimer), each of them including glycoconjugated and hydroxylated derivatives (Fig. 1). In the case of the *meta* and *para* groups we worked with tri- and tetra-substituted derivatives only, given that the mono- and di- substituted analogues are insoluble in water. One of the *para* derivatives bore spacers between the sugar and the TPP unit in order to increase sugar mobility [6]. Glycodendrimeric structure was designed in order to favor specific interactions with membrane receptors via a cluster effect [7].

The main objective of our work was to determine the impact of the above structural modifications on the lipophilicity of TPP derivatives and on their behavior in aqueous media in terms of self-aggregation and interaction with DMPC liposomes as a simple model of a lipid bilayer. Interactions with human serum albumin (HSA) were also studied, as this protein is one of the key compounds for drug distribution in human blood. The analysis was performed using techniques such as steady state and time resolved fluorescence emission spectroscopy, fluorescence anisotropy and fluorescence quenching.

2. Materials and methods

2.1. Materials

Nine derivatives of TPP were studied (Fig. 1). 5,10,15,20-*meso*-tetra-(*meta*-hydroxyphenyl) porphyrin [***m*-THPP**], and 5,10,15,20-*meso*-tetra-(*para*-hydroxyphenyl) porphyrin [***p*-THPP**] were prepared according to Bonnett et al. [22]. *Meta*-glycoconjugated derivatives 5,10,15-*meso*-tri-(*meta*-O-β-D-glucosyloxyphenyl)-20-phenyl porphyrin [**TPP(*m*-GluOH)$_3$**], 5,10,15,20-*meso*-tetra-(*meta*-O-β-D-glucosyloxyphenyl) porphyrin [**TPP(*m*-GluOH)$_4$**], and *para* glycoconjugated derivative 5,10,15,20-*meso*-tetra-(*para*-O-β-D-glucosyloxyphenyl) porphyrin [**TPP(*p*-GluOH)$_4$**], were prepared as described in our previous work [5,8], as well as 5,10,15-*meso*-tri(*para*-hydroxyphenyl)-20-phenylporphyrin [**TPP(*p*-OH)$_3$**] [23]. The synthesis of the glycosylated diethylene glycol porphyrin 5,10,15-tri{*para*-*O*-[2-((2-*O*-α-D-mannosyloxy)-ethoxy)-ethoxy]-phenyl}-20-phenyl porphyrin [**TPP(*p*-Deg-O-α-ManOH)$_3$**], was described in a more recent study [6]. Finally, two mono substituted derivatives bearing dendrimeric structure have been prepared [7], one glycoconjugated, **TPP-*p*-glycodendrimer**, and the other non-glycoconjugated, **TPP-*p*-dendrimer** (Fig. 1).

Dimyristoylphosphatidylcholine (DMPC, Mw = 677.9 g/mol), human serum albumin (HSA, essentially fatty acid free, 99% Mw = 66,500 g/mol [24]), sodium thiosulfate ($Na_2S_2O_3$) and potassium iodide (KI) were purchased from Sigma–Aldrich. Sodium hydroxide (NaOH), sodium dihydrogenophosphate (NaH_2PO_4), analytical grade chloroform, methanol and acetonitrile were provided by VWR International. All working solutions and liposome suspensions were prepared in a phosphate buffer saline (PBS) containing 0.01 M phosphate buffer, NaCl 0.138 M and KCl 2.7 mM (pH = 7.4) purchased from Sigma–Aldrich.

2.2. Preparation of liposomes

DMPC liposomes were prepared by the Bangham method followed by the extrusion of the vesicles suspensions [25]. A DMPC solution in chloroform:methanol (9:1, v/v) was evaporated under vacuum leaving a thin film on the flask wall. Phosphate buffer was added until the 4 mM DMPC concentration was reached and the film was peeled off by vortexing in the presence of glass beads. The milky aqueous suspension thus obtained was extruded through a 200 nm polycarbonate membrane filter at 50 °C using an extruder (Avestin Lipofast, Ottawa, California). After 10 extrusion cycles, the suspension turned into a homogeneous population of small unilamellar vesicles. The average liposome size (160 nm) was checked by photon correlation spectroscopy using a Coulter analyzer N4-MD (Coultronics, Margency, France).

2.3. Spectroscopy

- *Steady state spectroscopy*: UV–visible absorption measurements were carried out on a CARY 100 Bio UV–visible spectrophotometer (Varian, USA). Fluorescence emission spectra were recorded on a Perkin-Elmer LS-50B luminescence spectrometer (MA, USA) equipped with a red sensitive photomultiplier. Excitation of porphyrins was performed at the maximum of the Soret band. All samples had a low optical density (<0.05) at the wavelength of excitation in order to avoid the inner filter effects.
- *Time resolved fluorescence*: They were carried on a single photon counting set-up, based on a Titanium sapphire laser (Tsunami 3950B, Spectra Physics, Les Ulis, France) and a multi-channel plate photomultiplier (R3809U, Hamamatsu, Massy, France). Excitation of porphyrins was performed at 420 nm. For details of the experimental set-up see Schoutteten et al. [26].
- *Solutions*: 10^{-4} M porphyrin stock solution were prepared in methanol:pyridin (98:2, v/v) and directly diluted to 2×10^{-7} M in 0.01 M phosphate-buffered saline (PBS) just before the experiments. 1 mL porphyrin aqueous solutions were added to 1 mL of DMPC liposomes suspensions or HSA solution of various concentrations. The porphyrin concentration in the working solution was then 10^{-7} M. Higher porphyrin concentrations (2×10^{-7} M) were employed only for recording the absorption spectra in PBS and for time resolved fluorescence measurements. In all cases (except in the kinetics study) the samples were incubated for 24 h at 37 °C before measurements.

2.4. Association kinetics

In order to determine the incubation time required to reach equilibrium, the incorporation kinetics of the porphyrin into liposomes and HSA were studied at 37 °C using steady state fluorescence spectroscopy. The experiments were performed at a molar ratio of [DMPC]/[Porphyrin] and [HSA]/[Porphyrin] of 1000/1 in order to ensure complete porphyrin association. The variation of the intensity of porphyrin fluorescence emission was monitored with time.

2.5. Determination of porphyrin derivatives affinity for DMPC liposomes

Samples containing [DMPC]/[porphyrin] in various molar ratios (up to 1000/1) were prepared and kept at 37 °C in the dark for 24 h. The fluorescence emission was then measured at 37 °C.

The mathematical model: Porphyrin liposome/solution partition coefficients (K) can be determined using the approach introduced by Huang and Haugland [27]:

$$K = \frac{([L-P]/L)}{(P_f/W)} \quad (1)$$

where $[L-P]$, P_f, L, and W are the liposome-bound porphyrin, free porphyrin, phospholipid, and water concentrations respectively. The fluorescence intensity (F) of this system is then given by the equation:

$$\frac{(F-F_0)}{(F_{max}-F_0)} = \frac{[L-P]}{P} \quad (2)$$

wherein, F_0, and F_{max} are the fluorescence intensities of porphyrin measured in the lipid free solutions, and following complete association with the lipids, respectively. P is the total amount of the porphyrin: $P = [L-P] + P_f$. From Eqs. (1) and (2) we obtain:

$$F = F_0 + (F_{max} - F_0)(K/W)L/[1 + (K/W)L] \quad (3)$$

and Eq. (3) is fitted to the experimental data.

2.6. Determination of porphyrin derivatives association constant with albumin

As in the case of liposomes, [HSA]/[porphyrin] molar ratios were varied up to 1000/1; and fluorescence measurements were performed after incubation of the samples at 37 °C for 24 h.

The mathematical model: Albumin–porphyrin association is a complex feature, due to porphyrin and protein aggregation [28] and to the multiple binding sites of albumin [29,30]. In some cases, only a macroscopic association constant can be calculated. In our study, as HSA is in a large excess with respect to the porphyrin, we considered that only one binding site for porphyrin per albumin was actually effective [31] and we simplified the model to a 1:1 stoichiometry:

$$P + A \Leftrightarrow A - P \quad K_A = \frac{[A-P]}{P_f \; A} \quad (4)$$

The corresponding apparent association constant (K_A) could thus be determined by fitting the experimental data of fluorescence intensity (F) versus HSA concentration (A) to the equation:

$$F = F_0 + (F_{max} - F_0) K_A A/(1 + K_A A) \quad (5)$$

where F_0, and F_{max} are the fluorescence intensities of porphyrin measured in HSA free solutions, and after complete association with HSA, respectively.

2.7. Fluorescence quenching studies

A stock solution of 5 M KI was prepared in PBS, and 10^{-3} M $Na_2S_2O_3$ was added in order to prevent I_2 formation. In working solutions, the [DMPC]/[Porphyrin] molar ratio was 1000/1 to ensure total incorporation. After 24 h of incubation at 37 °C, small aliquots of KI stock solution were added to 2 mL of [Porphyrin]/[DMPC] solution, and then mixed. KI addition was performed at two different temperatures: 15 and 37 °C that is below and above respectively the DMPC phase transition temperature (23.5 °C)[32].

In both cases experimental data were fitted by the Stern–Volmer relationship:

$$I_0/I = \tau_0/\tau = 1 + \tau_0 k_q[KI] = 1 + K_{SV}[KI] \quad (6)$$

where I_0, I are the fluorescence intensities, τ_0, τ are the lifetimes of the excited state, in the absence and in the presence of the quencher respectively and k_q is the quenching rate constant. K_{SV} is the Stern–Volmer constant considering that a dynamic quenching mechanism is usually reported with I^- [33].

2.8. Fluorescence anisotropy

Steady state emission anisotropy (r) for liposome bound porphyrins was measured at 15 and 37 °C. Before measurements, porphyrins were incubated with a large excess of liposomes (1000/1: [DMPC]/[porphyrin]) during 24 h at 37 °C. It is worth noting that for the DMPC concentration used (10^{-4} M), light scattering occurred due to the size and number of DMPC vesicles and this artefact contributed to the total apparent fluorescence. In order to avoid this contribution, horizontal and vertical components of scattered light were carefully measured and subtracted from all measurements with liposomes. Excitation and emission wavelengths were chosen at the maximum of excitation and emission spectra of each derivative.

2.9. Competition between DMPC liposomes and HSA for porphyrin binding

(HSA–Porphyrin)–Liposomes interaction {(A–P)–L} or (Liposomes–Porphyrin)–HSA interaction {(L–P)–A}: HSA and porphyrin molecules or liposomes and porphyrin molecules, ([HSA]/[porphyrin] or [DMPC]/[porphyrin] molar ratio: 1000/1), were incubated in PBS at 37 °C in darkness for 24 h, and the fluorescence intensities were measured. Then, liposomes or HSA were added in the same ratio with respect to the porphyrin and incubated at 37 °C in darkness for another 24 h, and afterward the fluorescence intensities were recorded.

2.10. Lipophilicity evaluation

2.10.1. Experimental approach

The lipophilicity of the nine derivatives was studied by means of their retention time in an octadecyl stationary phase using reversed phase liquid chromatography (RP-LC).

- *Theoretical considerations*: Snyder and Dolan [34] have demonstrated that the retention time in a gradient (t_g) is:

$$t_g = (t_0/b)\,\log(2.3k_0b + 1) + t_0 + t_D \quad (7)$$

t_0 is the column dead time, t_D the system delay time and k_0 the retention factor of isocratic elution at the beginning of the gradient. b is defined as: $b = t_0 \times$ slope of the gradient $\times\, S$, where S is the slope in the linear strength model according to:

$$\log k = \log k_w - S\phi \quad (8)$$

with ϕ the organic solvent content in the mobile phase, and k_w the extrapolation of the retention in water. At the beginning of the gradient $\phi = \phi_0$ and $k = k_0$. Usually, $k_0\, b \gg 1$ and the logarithm term in Eq. (7) can be simplified. From Eqs. (7) and (8) the apparent retention factor $k_g = (t_g - t_0 - t_D)/t_0$ can be expressed as:

$$k_g = (1/b)(\log 2.3b + \log k_w - S\phi_0) \quad (9)$$

k_g is obviously linear function of $\log k_w$ and can be used to rank compounds in terms of lipophilicity. The same conclusions have been derived by Krass et al. [35].

- *Apparatus*: The HPLC equipment used was a BIO-TEK device consisting of a 525 gradient pump, 565 auto sampler, 582-column thermostat and 545 V diodes—array detector. The analytical column was an Uptisphere® ODB, (150 mm × 4.6 mm, 5 μm) purchased from Interchrom. Analysis was performed using gradient elution with a mobile phase varying from 5/95 (v/v) acetonitrile/water to 100% acetonitrile in 45 min with a total flow rate of 1 mL/min. Data acquisition and instrument control were carried out using the Kromasystem (Geminyx) 2000 software.

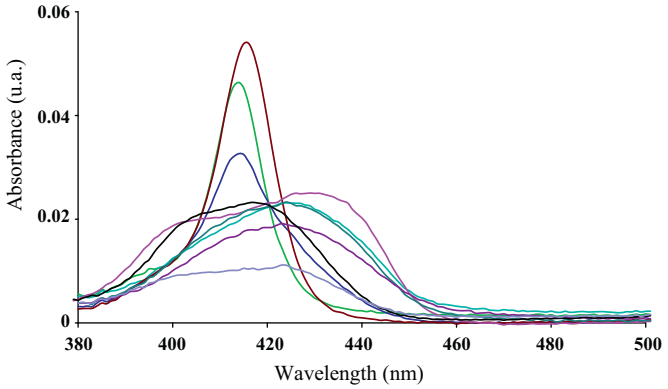

Fig. 2. Absorption spectra in PBS in Soret band region; [porphyrin] = 2×10^{-7} M. ( ), TPP(*m*-GluOH)$_4$; ( ), TPP(*m*-GluOH)$_3$; ( ), *m*-THPP; ( ), TPP(*p*-GluOH)$_4$; ( ), TPP(*p*-Deg-O-α-ManOH)$_3$; ( ), *p*-THPP; ( ), TPP(*p*-OH)$_3$; ( ), TPP-*p*-glycodendrimer; ( ), TPP-*p*-dendrimer.

2.10.2. In silico approach

The lipophilicity of the studied compounds was estimated by calculating log *P* values using appropriate software programs, such as ChemDraw Ultra 6.0 (CambridgeSoft.Com) and Calculator Plugins (MarvinBeans 4.1.13) from ChemAxon.

2.11. Molecular graphics

Molecular graphics were created using VMD—Visual Molecular Dynamics software [36]. DMPC bilayer coordinates were taken from the Biocomputing site of the University of Calgary [37] and porphyrin structures were generated using the Corina software [38].

3. Results and discussion

3.1. Self-aggregation in aqueous media and lipophilicity of porphyrin derivatives

Auto-association of porphyrin derivatives in aqueous media is very common and has been described by numerous authors [21,39]. According to Hunter and Sanders this feature is mainly due to π–σ interactions between the tetrapyrrolic macrocycles [40]. Aggregation induces important modifications on porphyrins absorption spectra: the maximum of the Soret band (the main absorption band) is red or blue shifted, associated with enlarged bands of lower intensity. The self-assembling of the porphyrin units is rather complex and can involve the formation of dimers, trimers, oligomers and/or large-scale aggregates.

The spectra of the monomer form of all compounds in methanol were characterized by a narrow Soret band centered between 414 and 417 nm (Table 1). The two symmetric compounds TPP(*p*-GluOH)$_4$ and TPP(*m*-GluOH)$_4$ were the only ones to exhibit a rather sharp Soret band in aqueous media (Fig. 2). Their absorption maximum was slightly blue shifted in PBS with respect to their monomer spectra in methanol (Table 1), probably due to the presence of dimers of face-to-face geometry (H-type aggregates) as already suggested for TPP(*p*-GluOH)$_4$ by other authors [39]. A broadening of the Soret band was observed for the asymmetric TPP(*m*-GluOH)$_3$, leading, at higher concentrations, to a red shift

Table 1
Comparison of lipophilicity, aggregation in aqueous media and binding to biomolecules for the nine studied derivatives. $\lambda_{methanol}$ and λ_{PBS} (nm) are the maximum of the Soret band in methanol and aqueous PBS respectively. k_g is the apparent retention factor for gradient elution in RP-LC ($n = 3$, RSD < 3%; $T = 22\,^{\circ}C$). Liposome/aqueous phase partition coefficient (K) and association constant with HSA (K_A) were determined at $T = 37\,^{\circ}C$.

Porphyrins	Aggregation		Lipophilicity	Liposomes binding	Albumin binding
	$\lambda_{methanol}$	λ_{PBS}	k_g	K ($\times 10^6$)	K_A ($\times 10^5$)
TPP(*m*-GluOH)$_4$	414.5	413	6.9	3.9 ± 0.5	214 ± 17
TPP(*m*-GluOH)$_3$	413.5	414	11.7	12.6 ± 0.9	10.1 ± 1.4
m-THPP	414.5	425	24.9	118 ± 20	6.0 ± 0.3
TPP(*p*-GluOH)$_4$	416	415	4.2	NA[a]	NA[a]
TPP(*p*-Deg-O-α-ManOH)$_3$	416	431 and 406	13.6	7.0 ± 0.7	0.33 ± 0.02
p-THPP	417	423	21.5	91 ± 16	15.8 ± 1.2
TPP(*p*-OH)$_3$	417	425	27.9	40.2 ± 1.8	5.2 ± 0.8
TPP-*p*-glycodendrimer	413	417 and 408	20.8	9.3 ± 0.7	1.6 ± 0.1
TPP-*p*-dendrimer	413	Very broad	29.1	11.6 ± 0.9	0.92 ± 0.06

[a] Not available.

probably due to an offset between the two macrocycles (J-type aggregates [41]). For all the other compounds, self-association in aqueous media was extensive. The hydroxylated compounds: *m*-THPP, *p*-THPP and TPP(*p*-OH)$_3$ showed quite similar absorption spectra with a very large Soret band and a pronounced red shift with respect to the spectra of their respective monomers. Bonnett et al. in their study of *m*-THPC, a photosensitizer having very close structure to that of *m*-THPP, have observed similar effects and attributed them to the contribution of edge-to-edge porphyrin arrangements (J-aggregates) involving hydrogen bonds between adjacent phenolic functions [42]. For TPP(*p*-Deg-O-α-ManOH)$_3$ and TPP-*p*-glycodendrimer, derivatives with particularly bulky substituents, the Soret band was split into two bands, one red shifted and one blue shifted with respect to the spectrum of the monomer (Fig. 2). The structure of the aggregates was difficult to deduce from these results; perhaps an oblique arrangement of porphyrin transition dipoles took place [43,44]. The absorbance of TPP-*p*-dendrimer was very low, indicating low water solubility.

In terms of lipophilicity, if we could easily classify derivatives of a same series (for example the three *meta*), we could not directly compare compounds of different series, for example a *meta* derivative and a dendrimer. However, it was necessary to determine whether there was any correlation between lipophilicity of porphyrin derivatives, their aggregation in aqueous media and their association with biomolecules. Lipophilicity of a drug is commonly evaluated by the octanol–water partition coefficient (log *P*), determined using the shake flask method. Nevertheless, due to their amphiphilic character and their aggregation in aqueous media, this method was not suitable for our compounds. On the other hand, computation using in silico approach (see experimental) cannot distinguish between *meta* and *para* substitution and give the same value not only for *m*-THPP and *p*-THPP but also for TPP(*m*-GluOH)$_4$ and TPP(*p*-GluOH)$_4$. For these reasons, we chose to evaluate the lipophilicity of the nine derivatives by monitoring their retention in reversed phase liquid chromatography (RP-LC) on a hydrophobic octadecyl stationary phase (Table 1).

As expected, glycoconjugation induced a decrease in the apparent retention factor (k_g), indicating more polar compounds (Table 1). We could also observe that the *para* derivatives *p*-THPP and TPP(*p*-GluOH)$_4$ behaved as more polar than the *meta* analogues *m*-THPP and TPP(*m*-GluOH)$_4$ as they exhibited shorter retentions. TPP(*p*-Deg-O-α-ManOH)$_3$ appeared slightly more hydrophobic than TPP(*m*-GluOH)$_3$, TPP-*p*-glycodendrimer showed a retention factor slightly below that of the two tetrahydroxylated derivatives *m*-THPP and *p*-THPP, and TPP-*p*-dendrimer seemed to be the least polar of all studied compounds (Table 1).

Self-association in solution was obviously a function of porphyrin lipophilicity. The two more polar studied compounds TPP(*p*-GluOH)$_4$ and TPP(*m*-GluOH)$_4$ exhibited high absorbance in PBS, with a rather sharp Soret band, demonstrating limited aggregation in aqueous media. The lowest absorbance value, corresponding to extensive aggregation and poor water solubility, was observed for the TPP-*p*-dendrimer.

3.2. Association kinetic studies with HSA and liposomes

Tri- and tetra-glycoconjugated *meta* derivatives [TPP(*m*-GluOH)$_3$ and TPP(*m*-GluOH)$_4$], that presented limited self-aggregation in solution, associated very rapidly to liposomes and HSA as shown by the constant fluorescence emission recorded immediately after their mixing (Fig. 3a and b). A slight decrease in intensity with time was observed. The fluorescence emission of the tetraglycoconjugated *para* derivative TPP(*p*-GluOH)$_4$, the most polar compound in this study, decreased very rapidly in

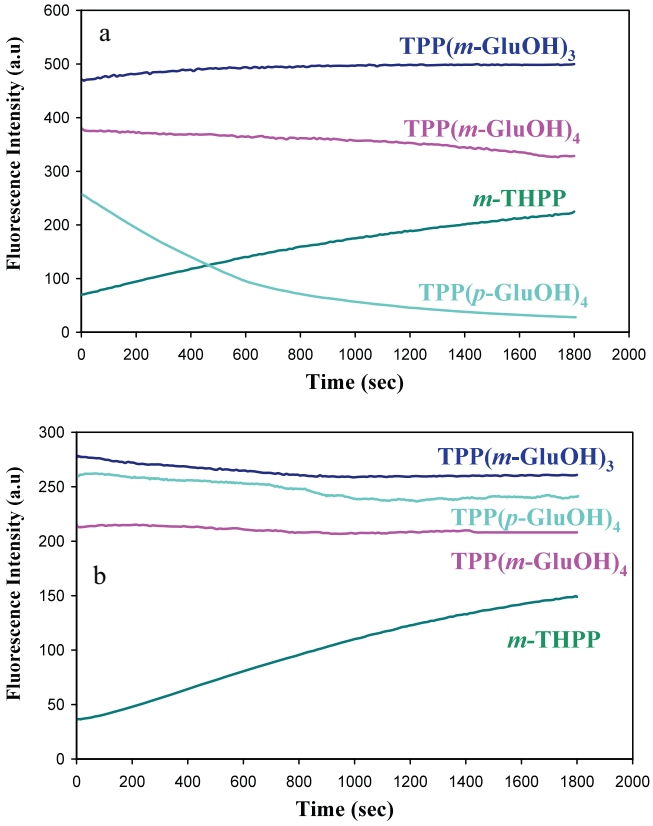

Fig. 3. Evolution of the emission intensity the first 30 min after mixing, (a) in the presence of liposomes, (b) in the presence of HSA. $T = 37\,^{\circ}C$, [DMPC] = 10^{-4} M, [HSA] = 10^{-4} M, [porphyrin] = 10^{-7} M.

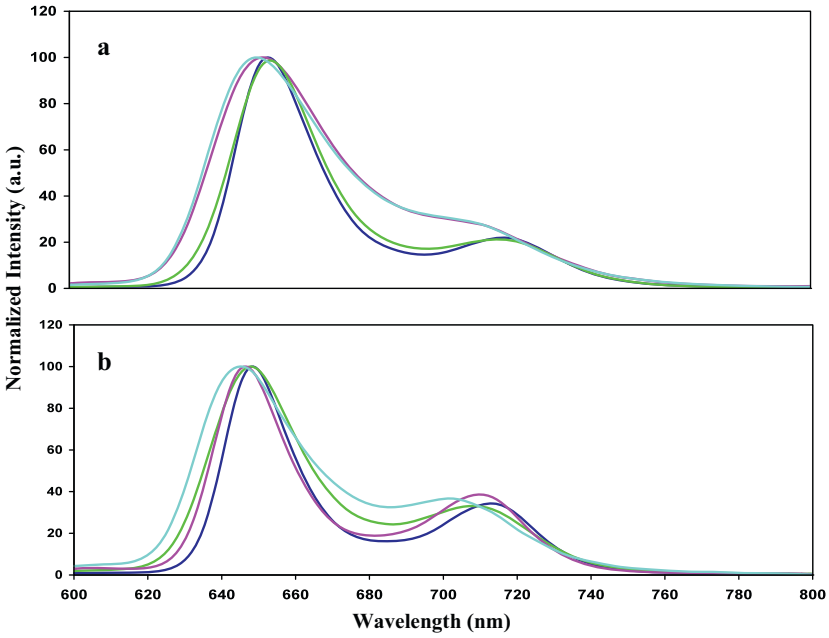

Fig. 4. Normalised fluorescence spectra of (a) TPP (*p*-GluOH)$_4$, (b) TPP (*m*-GluOH)$_4$ after 24 h of incubation at 37 °C in: ( ), PBS; ( ), DMPC; ( ), HSA, and ( ), Methanol, [porphyrin] = 10^{-7} M, [DMPC] = 10^{-4} M, [HSA] = 10^{-4} M.

the aqueous liposome suspension (Fig. 3a).[1] Normalized fluorescence spectra of TPP(*p*-GluOH)$_4$ remained the same as in PBS solution (Fig. 4a), indicating that no association with liposomes took place. Conversely, TPP(*p*-GluOH)$_4$ presented a rapid association with albumin with a slight fluorescence emission decrease with time (Fig. 3b). In the presence of HSA, its spectrum became similar to that of its monomer in methanol (Fig. 4a), accounting for the association.

For all compounds except TPP(*p*-GluOH)$_4$, normalized fluorescence spectra in the presence of liposomes or HSA were quite different from those in aqueous PBS accounting, with the increase in fluorescence intensity, for porphyrin binding (example TPP(*m*-GluOH)$_4$, Fig. 4b).

The derivatives showing a large self-association in PBS (*m*-THPP, *p*-THPP, TPP(*p*-Deg-O-α-ManOH)$_3$, TPP(*p*-OH)$_3$ and the two dendrimers), also presented slow association rates with HSA and liposomes. As an example, we show the association of *m*-THPP in Fig. 3a and b: fluorescence emission was still rising 30 min after mixing and the plateau was actually reached after 6 h only (data not shown). For all derivatives exhibiting slow kinetics, equilibrium was reached within 8 h, and the fluorescence intensity remained constant for the following 24 h.

Association of porphyrins to HSA or liposomes was expected to be a two-steps process: firstly dissociation of the aggregates and secondly, binding of monomers to albumin or liposomes. We observed that for all compounds (except TPP(*p*-GluOH)$_4$) kinetics were rather similar for liposomes and HSA, suggesting that the break-up process of porphyrin aggregates was the limiting step.

3.3. Affinity for liposomes and albumin

As mentioned above, addition of HSA or DMPC liposomes in PBS induced a progressive dissociation of porphyrin aggregates with regeneration of porphyrin monomer fluorescence emission, until saturation occurred in the presence of an excess of liposomes (Fig. 5a) or HSA.

The liposome-aqueous phase partition coefficient (*K*) (Table 1) decreased with increasing glycoconjugation and this was verified for the three series of studied derivatives. For example, the partition coefficient of the *meta* derivatives decreased in the order: *m*-THPP > TPP(*m*-GluOH)$_3$ > TPP(*m*-GluOH)$_4$. For *para* derivatives, as we have demonstrated in the previous paragraph, TPP(*p*-GluOH)$_4$

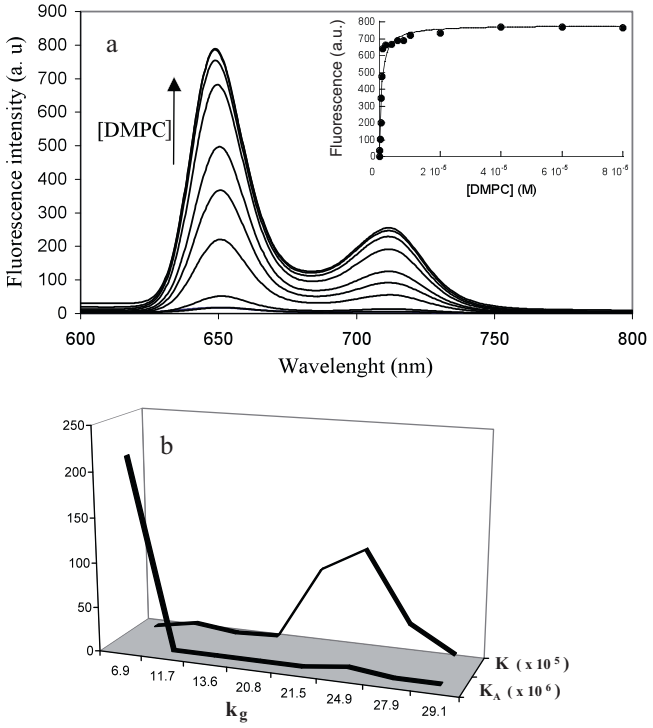

Fig. 5. (a) Evolution of fluorescence emission of *m*-THPP as a function of DMPC concentration, [*m*-THPP] = 10^{-7} M. (b) Evolution of liposome/aqueous phase partition coefficient (*K*) and of association constant with HSA (K_A) as a function of the apparent retention factor k_g.

[1] Decrease of emission with time for free porphyrin (not associated with liposomes or albumin) in aqueous media has already be reported for other porphyrin derivatives and is related to their low solubility.

Table 2
Fluorescence life times of the nine compounds dissolved in methanol at 22 °C (τ_m) and bound to liposomes (τ_L) at 37 °C and at 15 °C in the absence of the quencher. K_{SV} is the slope of Stern–Volmer plots, and k_q the quenching rate constant ($k_q = K_{SV}/\tau_L$).

Porphyrin	τ_m (ns) 22 °C	Quenching in liposome suspension at 37 °C			Quenching in liposome suspension at 15 °C		
		K_{SV} (M^{-1})	τ_L (ns)	k_q (M^{-1} s^{-1}) $\times 10^8$	K_{SV} (M^{-1})	τ_L (ns)	k_q (M^{-1} s^{-1}) $\times 10^8$
TPP(*m*-GluOH)$_4$	9.9	6.5 ± 0.08	11.3	5.8 ± 0.07	5.1 ± 0.10	12.0	4.3 ± 0.09
TPP(*m*-GluOH)$_3$	9.4	3.4 ± 0.06	11.4	3.0 ± 0.05	4.3 ± 0.11	11.9	3.6 ± 0.09
m-THPP	9.0	4.6 ± 0.11	10.6	4.3 ± 0.09	2.8 ± 0.07	11.1	2.9 ± 0.09
TPP(*p*-GluOH)$_4$	8.9		8.14			8.14	
TPP(*p*-Deg-O-α-ManOH)$_3$	8.6	1.3 ± 0.04	10.8	1.2 ± 0.04	3.6 ± 0.08	10.6	3.4 ± 0.08
TPP(*p*-OH)$_3$	8.0	1.7 ± 0.08	9.26	1.8 ± 0.09	3.1 ± 0.10	9.50	3.3 ± 0.10
p-THPP	8.2	4.1 ± 0.13	8.75	4.7 ± 0.15	4.4 ± 0.10	8.90	4.9 ± 0.11
TPP-*p*-glycodendrimer	9.4	0.47 ± 0.02	12.3	0.38 ± 0.01	1.4 ± 0.03	12.7	1.1 ± 0.02
TPP-*p*-dendrimer	9.5	0.32 ± 0.01	12.3	0.28 ± 0.01	1.1 ± 0.03	12.8	0.90 ± 0.02

did not bind to liposomes at all. The triglycoconjugated derivative TPP(*p*-Deg-O-α-ManOH)$_3$ bound to liposomes but presented a lower affinity than the non-glycoconjugated TPP(*p*-OH)$_3$. The TPP-*p*-glycodendrimer also showed a lower affinity than its non-glycoconjugated parent compound.

An opposite trend was observed for the association of porphyrins with HSA: for *meta* derivatives and for the dendrimer compounds (Table 1), a significant increase of the association constant (K_A) was induced by the glycoconjugation. In contrast, the *para* derivative TPP(*p*-Deg-O-α-ManOH)$_3$ presented low affinity for HSA, even lower than the non-glycoconjugated TPP(*p*-OH)$_3$, probably due to the presence of the diethylene glycol spacer. Whereas it did not bind to liposomes, TPP (*p*-GluOH)$_4$ appeared able to bind to HSA. Unfortunately, accurate determination of its K_A was impossible due to the limited enhancement of fluorescence intensity induced by this association.

As we have mentioned before, chromatographic retention experiments demonstrated that the *para* derivatives *p*-THPP and TPP(*p*-GluOH)$_4$ were more polar than the *meta* analogues: *m*-THPP and TPP(*m*-GluOH)$_4$. This can be correlated with their lower affinity for liposomes. However, it is not possible in all cases to correlate increased polarity to a decreased affinity for liposomes. Indeed, TPP(*p*-Deg-O-α-ManOH)$_3$ was less polar than TPP(*m*-GluOH)$_3$, but it showed a lower *K* value. Similarly, partition coefficients of dendrimer compounds were in the same order of magnitude than the tri-substituted derivatives TPP(*m*-GluOH)$_3$ and TPP(*p*-Deg-O-α-ManOH)$_3$ in spite of their lipophilicity. It is noteworthy, as we observe in Fig. 5b, that the affinity for liposomes was optimum for derivatives having intermediate value of k_g. This apparent discrepancy between porphyrin lipophilicity and their affinity for liposomes could be explained by the fact that the classification of the compounds by their retention time only takes into account their interaction with aliphatic chains. Yet, to associate with liposomes, porphyrin derivatives would have to penetrate first the polar head groups region of phospholipids. From this point of view, it is not surprising that the highest binding constants were obtained for hydroxylated derivatives exhibiting intermediate lipophilicity.

3.4. Porphyrin localization in liposomes

3.4.1. Time resolved fluorescence spectroscopy

When DMPC vesicles were in large excess, porphyrin could be considered as entirely bound to them. The fluorescence lifetimes τ of the porphyrins were measured by time resolved fluorescence spectroscopy at +15 °C and +37 °C. For all components mono exponential decays were observed (see for example TPP(*m*-GluOH)$_4$ curve 1, Fig. 6) demonstrating the presence of only one fluorescent species bound to liposomes. The obtained values were close to lifetimes measured for the same compounds in methanol (Table 2) indicating that porphyrins were bound in their monomer form.

Cooling from 37 °C to 15 °C induced an increase in the lifetime values τ for all compounds except for TPP(*p*-Deg-O-α-ManOH)$_3$. The observed higher values at 15 °C were probably due to slower non-radiative rates (k_{nr}) at lower temperature.

3.4.2. Dynamic fluorescence quenching

I^- is a quencher known to penetrate to some extent itself, into phospholipid bilayers forming a concentration gradient [45,46]. Its use has become the simplest way to obtain information about the relative penetration depth of membrane-bound fluorophores including porphyrins [47]. In this work we compared the relative depths of penetration of 8 porphyrins into DMPC bilayer by means of the quenching rate constants (k_q) with iodide. k_q values can be calculated from the Stern–Volmer (K_{SV}) constants of porphyrin bound to liposomes and the lifetime values in the absence of the quencher (Eq. (6)). Quenching by iodide (I^-) led to linear plots for all studied compounds (Fig. 7). Deviations from linearity have been previously reported in the literature and were attributed to the presence of different porphyrin populations with various accessibilities to the quencher [9,11]. However, in our experiments, the deviations from linearity remained within the experimental error. The shape and the maximum of porphyrin absorption spectra remained the same in the presence of the quencher (results not shown) and the lifetime of the excited state decreased (for example TPP(*m*-GluOH)$_4$, Fig. 6) in agreement with a dynamic quenching process.

At 37 °C, high values of K_{SV} and k_q were obtained for the three tetra-substituted compounds *m*-THPP, *p*-THPP and TPP(*m*-GluOH)$_4$ (Table 2). The highest values were observed for the latter,

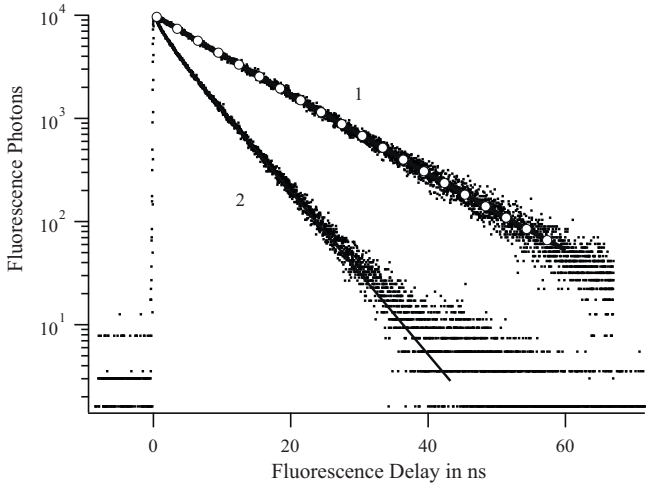

Fig. 6. Fluorescence decay of TPP(*m*-GluOH)$_4$ bound to liposomes at 37 °C; [TPP(*m*-GluOH)$_4$] = 2×10^{-7} M. Curve 1 without the quencher, curve 2 in the presence of [I^-] = 0.5 M.

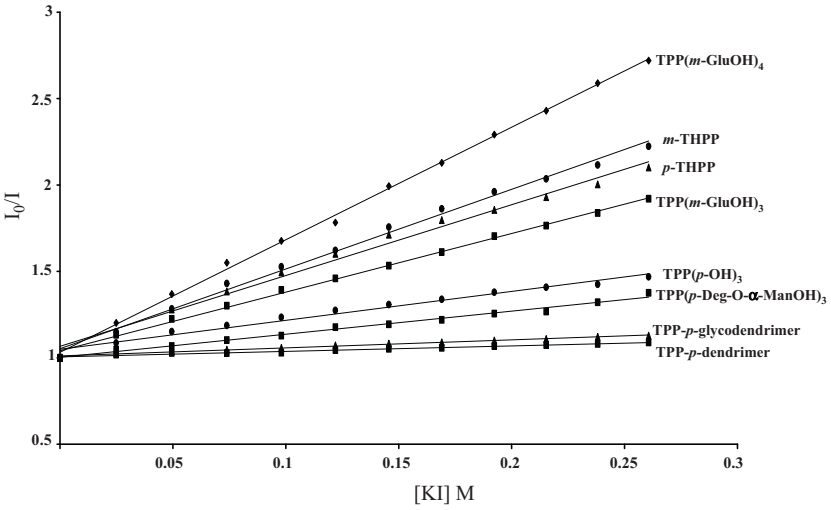

Fig. 7. Stern–Volmer plot of bound porphyrins at 37 °C, [DMPC] = 10^{-4} M, [porphyrin] = 10^{-7} M.

suggesting that this compound was located near or within the polar head group region of the phospholipid bilayer, where it could be more easily quenched by I^-. Tetra-substituted compounds bearing hydroxyl units instead of sugars (*m*-THPP, *p*-THPP) presented lower k_q than TPP(*m*-GluOH)$_4$. Tri-substituted compounds presented lower inhibition constants than tetra-substituted ones, which could indicate that they were located deeper into the phospholipid bilayer. Thus, TPP(*m*-GluOH)$_3$ was deeper inserted into the bilayer than *m*-THPP and *p*-THPP, in spite of its more voluminous substituents grafted on the phenyl groups. We also observed that the presence of the diethylene glycol spacer in TPP(*p*-Deg-O-α-ManOH)$_3$ favoured TPP penetration between the aliphatic chains. It is worth noting that this compound was even deeper inserted in the bilayer than TPP(*p*-OH)$_3$. The lowest inhibition rate constants were obtained for the dendrimers (Fig. 7, Table 2), which were apparently the molecules that penetrated the most deeply into liposome bilayers. On the basis of these results it is evident that the depth of penetration into the phospholipid bilayer increased with increasing number of free apolar phenyl units.

When the temperature decreased from 37 to 15 °C the phospholipid hydrophobic chains became rigid. The work of Langner and Hui [46] has shown that inhibition constants by iodide of fluorophore embedded into hydrophobic chains of DMPC bilayer were slightly higher at 15 °C than at 37 °C. This was indeed the case for the trisubstituted derivatives and the dendrimers in our study (Table 2). The increase was significant for TPP(*p*-Deg-O-α-ManOH)$_3$ and TPP(*p*-OH)$_3$, suggesting that in a rigid monolayer, these compounds were partially displaced towards the polar region. The tetra-substituted compounds located in the polar region of the bilayer presented unchanged (*p*-THPP) or decreased (*m*-THPP and TPP(*m*-GluOH)$_4$) k_q values, probably induced by lower diffusion coefficients of iodide at lower temperature.

In order to prove the protective effect of the liposome, many authors [9,47] have compared the quenching constant K_{SV} obtained with iodide, when a porphyrin was bound to liposomes or free in the bulk solution. In our case no useful information could be deduced from this comparison as the studied derivatives aggregated in buffer making it impossible to study the quenching of the monomers in aqueous media. Stern–Volmer plots of the aggregates have been established however, for the three derivatives that had limited aggregation in PBS: TPP(*p*-GluOH)$_4$, TPP(*m*-GluOH)$_3$ and TPP(*m*-GluOH)$_4$. K_{SV} was 15 M^{-1} for TPP(*m*-GluOH)$_3$, but as high as 50 M^{-1} for the two others. For all three compounds these values were much higher than those obtained in liposomes. For the other compounds, random deviations from linearity without a particular pattern have been observed; these features were attributed to modification of porphyrins aggregates induced by iodide.

3.4.3. Steady state fluorescence anisotropy

Anisotropy values of the nine compounds were very low in methanol (Table 3) due to rotational depolarization. Associated with liposomes, all porphyrins presented values closer to those reported in glycerol, indicating a rigid microenvironment especially at 15 °C, below the transition temperature. The anisotropy values in liposomes were between 0.02 and 0.08 (Table 3) in agreement with the values obtained for some other TPP derivatives in DMPC liposomes [16].[2] Conversely, for TPP(*p*-GluOH)$_4$, anisotropy values were 0.147 and 0.26 at 37 and 15 °C respectively; as this compound did not bind to liposomes, these values correspond to its aggregates in PBS [48,49]. Cooling from 37 °C to 15 °C induced the most significant increase in the anisotropy value for TPP(*p*-Deg-O-α-ManOH)$_3$ and the two dendrimer compounds (see Table 3), suggesting that these three compounds were located deep in the phospholipid bilayer as the changes in microviscosity are reported to be more significant near the center of the bilayer [50].

3.4.4. Temperature effect in fluorescence emission

The steady state fluorescence intensity was monitored during the cooling from 37 to 15 °C. In the absence of porphyrins, the phase transition was determined from the intensity trend of the scattering light (Fig. 8a). The transition temperature corresponds to the inflection point of the curve, that is 25.5 °C for the scattering light curve. This value is close to the DMPC transition temperature reported in the literature, determined by differential scanning calorimetry (23.5 °C)[32], and to the value determined for large DMPC liposomes using 1,6-diphenyl hexatriene (DPH) as a probe (24.4 °C)[51]. Porphyrins emission intensity increased gradually with decreasing temperature, and presented a steep increase near the phase transition (see Fig. 8b,c,d). Similar curves to that of *m*-THPP presented in Fig. 8b were obtained for *p*-THPP, TPP(*m*-GluOH)$_3$, and TPP(*p*-OH)$_3$. For TPP(*m*-GluOH)$_4$ the transition curve was also similar but shifted by −0.8 °C. These results suggest that all these derivatives (at least

[2] High values of polarization could be obtained with excitation at the QX00 band (~630 nm for TPP derivatives). In our conditions, porphyrin concentrations make that significant emission intensities could be recorded only after excitation at the maximum of the main band (Soret band).

Table 3
Steady state fluorescence anisotropy values (r) of porphyrins in various media. (SD ≤ 0.003). % Δr is the anisotropy increase in % from 37 °C to 15 °C.

Porphyrins	Methanol (22 °C)	Glycerol (22 °C)	Liposomes (37 °C)	Liposomes (15 °C)	% Δr (15–37 °C)
TPP(m-GluOH)$_4$	0.006	0.066	0.070	0.080	13
TPP(m-GluOH)$_3$	0.001	0.070	0.050	0.060	17
m-THPP	0.001	0.066	0.050	0.056	11
TPP(p-GluOH)$_4$	0.004	0.071	0.148	0.269	
TPP(p-Deg-O-α-ManOH)$_3$	0.008	0.096	0.037	0.058	36
TPP(p-OH)$_3$	0.004	0.089	0.040	0.055	27
p-THPP	0.004	0.077	0.035	0.037	5
TPP-p-glycodendrimer	0.008	0.082	0.033	0.052	37
TPP-p-dendrimer	0.004	0.087	0.024	0.048	50

a significant fraction), including the most hydrophilic tetra glycoconjugated TPP(m-GluOH)$_4$, were not located outside the bilayer but inside (in the polar or in the hydrophobic region depending on the depth of penetration). We know from quenching experiments that TPP(p-Deg-O-α-ManOH)$_3$ and the dendrimers are the most deeply inserted compounds. For TPP(p-Deg-O-α-ManOH)$_3$, the phase transition to the gel phase induced a meaningful fluorescence enhancement and shift of −2 °C (Fig. 8c). In contrast, for the dendrimer compounds, the steep increase observed in fluorescence emission was of the same order (in absolute intensity values) as that of the scattering light, and almost undistinguishable in the normalised curve (Fig. 8d), despite the fact that these compounds were the two most deeply inserted into the bilayer.

After cooling from 37 °C to 15 °C, the fluorescence was recorded as the temperature was raised from 15 °C to 37 °C. For all studied derivatives, the obtained curves were exactly surimposable on the cooling curves, demonstrating that the observed phenomenon was reversible.

3.4.5. Molecular graphics

The depth of penetration of the different porphyrin derivatives as described in the previous paragraph was assessed using fluorescence quenching and fluorescence anisotropy. Based on these results and on structural considerations, molecular graphic of glycoconjugated porphyrins localization at the level of DMPC polar headgroups or in the region of hydrophobic chains is proposed in Fig. 9. DMPC bilayer structure and conformation were taken from Tieleman [37]. The hydrophobic TPP unit in TPP(m-GluOH)$_4$, surrounded by four sugars, would not penetrate into the aliphatic chain region. As already suggested in a previous work [52], this derivative was located at the level of the choline and glycerol groups of the bilayer. Conversely, the asymmetric TPP(m-GluOH)$_3$, due to its free phenyl group could be inserted into the aliphatic chain region. The presence of a spacer between the phenyl group and the sugar in TPP(p-Deg-O-α-ManOH)$_3$ would increase the flexibility of the sugars and allow the molecule adopting conformations favourable to a deeper penetration into the bilayer. Finally, for the dendrimer compounds, the entire TPP unit would be inserted into the aliphatic chain region with the amide link into the glycerol region. The TPP-p-glycodendrimer would be localised deeply into the hydrophobic chain region with the two opposite phenyl groups in the region between the two phospholipid leaflets (Fig. 9).

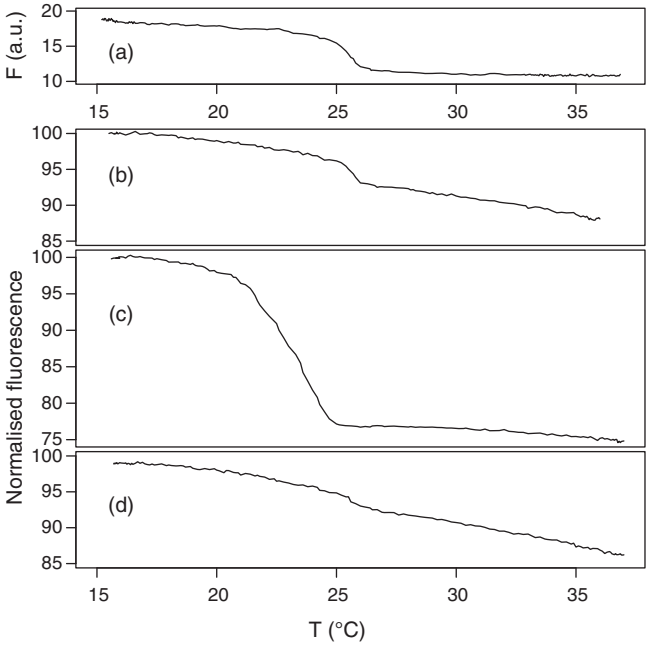

Fig. 8. (a) Intensity of scattered light (F) at 650 nm during cooling, excitation at 420 nm; (b), (c), (d) normalized emission intensity at the wavelength of the maximum emission of each porphyrin, excitation at the maximum of the Soret band. (b): m-THPP, (c): TPP(p-Deg-O-α-ManOH)$_3$, (d): TPP-p-dendrimer.

3.4.6. Concluding remarks

It is worth noting that the relative depths of penetration established by the inhibition study illustrated in Fig. 7 are in excellent agreement with the lifetime and anisotropy measurements. Lifetime of fluorophores was reported to increase with the depth of penetration into a phospholipid bilayer [53]. The lifetime increase in liposomes, with respect to methanol, was more significant for the compounds deeply inserted into the bilayer, e.g. 30% for the dendrimers and only 7% for p-THPP (values calculated from Table 2). There was also an excellent correlation between the k_q values at 37 °C (Table 2) and the impact of the temperature on fluorescence anisotropy (% Δr, Table 3). For example, the porphyrins located deeply into phospholipids bilayer had small k_q values and presented a high anisotropy increase % Δr upon cooling. The opposite was observed for the derivatives located in the headgroup region. k_q and % Δr were highly correlated (calculated correlation coefficient $R^2 = 0.88$).

On another hand, the knowledge of photosensitizer localization in DMPC bilayer helps us to better understand the transition curves of TPP(p-Deg-O-α-ManOH)$_3$ and TPP-p-dendrimer (Fig. 8). It is known that the contribution of radiative (k_r) and non-radiative (k_{nr}) to the overall decay of porphyrins is a function of the interactions between the tetrapyrrolic macrocycle and the phenyl groups at the meso position as well as a function of the distortion of the macrocycle [54]. For the dendrimer derivatives, the decrease in the available space during condensation had the smallest disturbance on the phenyl–tetrapyrrolic macrocycle conformation, due to the location of the two opposite phenyl groups in the region between the two phospholipid leaflets: it can be the reason why no abrupt increase fluorescence has been observed with cooling (Fig. 8d). Conversely, because the three bulky substituents of TPP(p-Deg-O-α-ManOH)$_3$ interacted with the hydrophobic chains of the phospholipids, lipid

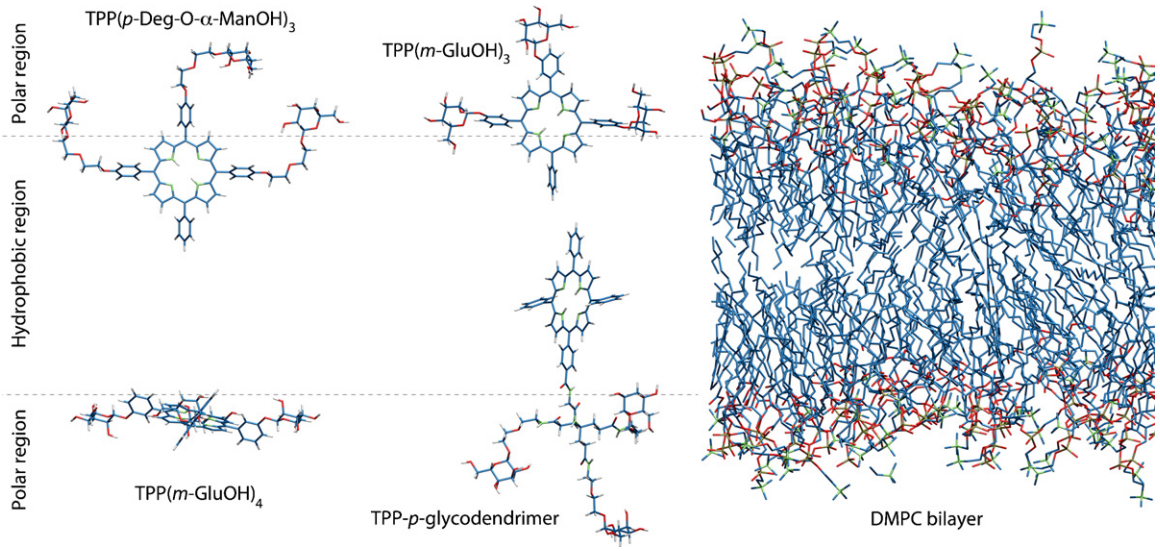

Fig. 9. Molecular graphics: depth of penetration of TPP derivatives into DMPC bilayer. Carbon: blue; Nitrogen: green, Oxygen: red. Structure of DMPC bilayer was obtained from Tieleman [37]. (For interpretation of the references to colour in this figure legend, the reader is referred to the web version of this article.)

condensation induced a change in the conformation of these substituents, reducing their mobility, affecting the planarity of the macrocycle and the angle between the phenyl group and the macrocycle. As the lifetime (τ) was lower at 15 °C for this compound (see Table 2), the increase of fluorescence could only be explained by increased radiative rate constants (k_r) ($\Phi_f = k_r\tau$) induced by changes in the conformation of the molecule. An important decrease in the transition temperature was also observed (Fig. 8c), demonstrating that this compound disturbed the phospholipid bilayer more than the others and locally fluidified it. This is in agreement with EPR studies, performed by other authors, demonstrating that maximum perturbing effect on membrane phase transition is induced when bulky groups are located at the middle of the alkyl chains [55].

3.5. Competition between DMPC liposomes and HSA for porphyrin binding

3.5.1. Spectral characteristics of bound porphyrin

As already mentioned, for all the compounds except TPP(*p*-GluOH)$_4$, normalized fluorescence spectra in the presence of liposomes or HSA were quite different from those in aqueous PBS, accounting for porphyrin binding. The spectra of bound porphyrins were not strictly similar to those recorded in methanol and could be different when they interacted with liposomes or HSA (example TPP(*m*-GluOH)$_4$, Fig. 4b, see also Supplementary information). The spectra showed some particularities, resulting from specific interactions, microenvironment polarity and change in conformation when the porphyrins were bound to liposome or albumin.

The spectral modifications observed were too small to allow studying specific porphyrin–biomolecule interactions, but they were quite reproducible. They could then be very useful to find the localization of porphyrin in more complex media, e.g. when studying the competition between liposome and albumin towards porphyrin binding.

3.5.2. Porphyrin binding competition

For all the compounds studied, the spectrum obtained following the {(A–P)–L} protocol was similar to that obtained with the second one {(L–P)–A} within experimental error. This indicates that porphyrin association with liposomes or HSA would be a reversible process, and that liposomes and HSA could compete for porphyrin binding.

It is reasonable to consider that two fluorescent species existed, one bound to HSA and the other one bound to liposomes. If x is the fraction of the porphyrin bound to liposomes, $1 - x$ will be the fraction bound to HSA. Then, the total fluorescence emission F_{L+A} of the system should be:

$$F_{L+A} = (1 - x)\ F_A + xF_L \quad (10)$$

The comparison with the fluorescence emission in the presence of only liposomes F_L or only albumin F_A allows (using Eq. (10)) to calculate the fraction x of the porphyrin bound to liposomes.

As it is mentioned in the kinetics study, the fluorescence emission of TPP(*m*-GluOH)$_4$ and TPP(*m*-GluOH)$_3$ decreased with time. Even if the signal decay was limited, the whole porphyrin concentration was not the same in all cases and accurate estimation of x could not be performed. Nevertheless, comparison of normalized excitation and emission spectra in the three media (L, A and mixture of them) suggests that the two compounds were mainly (>50%) bound to liposomes (see also Supplementary information).

Estimation of x demonstrates that the two tetra hydroxylated porphyrins (*m*-THPP and *p*-THPP) bound preferentially to liposomes to an extent of ~70%, this percentage being even higher (95%) for the trihydroxylated derivative TPP(*p*-OH)$_3$. Comparison of normalized excitation and emission spectra for each hydroxylated derivatives in the various media (L, A and L + A) confirmed the preferential binding to liposomes. TPP(*p*-Deg-O-α-ManOH)$_3$ had similar normalized emission spectra in liposomes and HSA but different excitation spectra; comparison of the excitation maximum then suggests a partition of the derivative between liposome and HSA. The calculation based on the differences in fluorescence emission intensity (using Eq. (10)) suggests that 60% of this derivative bound to liposomes.

Normalized spectra of dendrimers were similar in the presence of HSA and liposomes and the competition process could be studied only from the variations in fluorescence intensity. Using equation (10), the partition fraction in liposomes was evaluated to 56% for glycoconjugated dendrimer and 64% for the non-glycoconjugated.

To summarize, our results demonstrated that the competition process was dependent on the porphyrin structure. Nevertheless, for all studied compounds, except TPP(*p*-GluOH)$_4$, partitioning between liposomes and HSA took place, but the porphyrin was always mainly localized in the phospholipid bilayer.

4. Conclusion

In this work, three series of neutral tetraphenyl porphyrin (TPP) derivatives were compared with the main objective to evaluate the impact of structural modifications on porphyrin interactions with a phospholipid bilayer and with human serum albumin.

It was found that glycoconjugation of a tetraphenyl porphyrin unit increased the solubility of the compound in aqueous media, diminished its self-aggregation and induced very rapid kinetics of association with DMPC liposomes and HSA. However, glycoconjugation also decreased the liposome/aqueous phase partition coefficient (K) accounting for a diminution of porphyrin affinity for the phospholipid bilayer in all cases (*meta*, *para* and dendrimer derivatives). On the other hand, glycoconjugation seemed to increase the binding constant with albumin (K_A): the highest value of K_A has been observed for a tetra-glycoconjugated analogue, the TPP(*m*-GluOH)$_4$. The presence of a diethyl glycol spacer between the sugar and the TPP unit in the TPP(*p*-Deg-O-α-ManOH)$_3$ derivative led to a large self-aggregation in aqueous media and a low affinity, especially for albumin. The presence of hydroxyl groups grafted on the TPP macrocycle favoured its affinity for DMPC liposomes: the highest affinity was observed for the two tetra-hydroxylated derivatives, *m*-THPP and *p*-THPP. The position of the grafted group (*meta* or *para*) seemed also to have some importance: *para* derivatives presented lower affinity for liposomes than the corresponding *meta* bearing the same number and nature of substitution. Dendrimer structure derivatives presented large self-aggregation, and relatively low affinity for liposomes and albumin.

The lipophilicity of the porphyrins has been evaluated by their apparent retention (k_g) on an octadecyl stationary phase, and an attempt was made to correlate lipophilicity and affinity of the porphyrin for liposomes and albumin. It was observed that the derivatives presenting the highest affinity for DMPC liposomes (*m*-THPP and *p*-THPP) had intermediate lipophilicity; the derivative presenting the highest affinity for albumin (TPP(*m*-GluOH)$_4$) was the more polar one.

The depth of a TPP derivative penetration into the phospholipid bilayer mainly depends on the number of its free phenyl groups. This number is maximum for the dendrimers that have three free phenyl groups and these derivatives were the most deeply inserted into the hydrophobic chains region. Trisubstituted compounds have only one free phenyl group and penetrated to a lesser extent than the dendrimers. However, the presence of a diethylene glycol spacer increased the distance of the sugar from the phenyl group and thus, allowed insertion of the macrocycle deeper into the aliphatic chains. Tetrasubstituted compounds (*p*-THPP, *m*-THPP and TPP(*m*-GluOH)$_4$) that have no free phenyl group, were the less deeply inserted and apparently remained near the region of glycerol groups.

As a conclusion, the studied structural modifications induce major effects on the TPP derivatives aggregation and on their interactions with DMPC liposome and HSA. The knowledge of these effects could contribute to the better understanding of the behaviour of these derivatives in biological media.

Acknowledgments

The authors are grateful to Dr Ioannis Nicolis for his contribution to the molecular graphic constructions and to Mr. Ali Makky for the preparation of DMPC liposomes.

Appendix A. Supplementary data

Supplementary data associated with this article can be found, in the online version, at doi:10.1016/j.jphotochem.2010.09.008.

References

[1] S.K. Pushpan, S. Venkatraman, V.G. Anand, J. Sankar, D. Parmeswaran, S. Ganesan, T.K. Chandrashekar, Porphyrins in photodynamic therapy—a search for ideal photosensitizers, Curr. Med. Chem. Anticancer Agents 2 (2002) 187–207.
[2] R. Bonnett, Photosensitizers of the porphyrin and phthalocyanine series for photodynamic therapy, Chem. Soc. Rev. 24 (1995) 19–33.
[3] K. Berg, J.C. Bommer, J.W. Winkelman, J. Moan, Cellular uptake and relative efficiency in cell inactivation by photoactivated sulfonated meso-tetraphenylporphines, Photochem. Photobiol. 52 (1990) 775–781.
[4] I.J. MacDonald, J. Morgan, D.A. Bellnier, G.M. Paszkiewicz, J.E. Whitaker, D.J. Litchfield, T.J. Dougherty, Subcellular localization patterns and their relationship to photodynamic activity of pyropheophorbide-a derivatives, Photochem. Photobiol. 70 (1999) 789–797.
[5] D. Oulmi, P. Maillard, J.L. Guerquin-Kern, C. Huel, M. Momenteau, Glyconjugated porphyrins. 3 Synthesis of flat amphiphilic meso-(glycosylated-aryl)-aryl porphyrins and mixed meso-(glycosylated-aryl)-alkyl porphyrins bearing some mono and disaccharide groups, J. Org. Chem. 60 (1995) 1554–1564.
[6] I. Laville, S. Pigaglio, J.C. Blais, F. Doz, B. Loock, P. Maillard, D.S. Grierson, J. Blais, Photodynamic efficiency of diethylene glycol-linked glycoconjugated porphyrins in human retinoblastoma cells, J. Med. Chem. 49 (2006) 2558–2567.
[7] S. Ballut, A. Makky, B. Loock, J.P. Michel, P. Maillard, V. Rosilio, New strategy for targeting of photosensitizers. Synthesis of glycodendrimeric phenylporphyrins, incorporation into a liposome membrane and interaction with a specific lectin, Chem. Commun. (2009) 224–226.
[8] I. Laville, T. Figueiredo, B. Loock, S. Pigaglio, P. Maillard, D.S. Grierson, D. Carrez, A. Croisy, J. Blais, Synthesis, cellular internalization and photodynamic activity of glucoconjugated derivatives of tri and tetra(meta-hydroxyphenyl)chlorins, Bioorg. Med. Chem. 11 (2003) 1643–1652.
[9] F. Ricchelli, G. Jori, Distribution of porphyrins in the various compartments of unilamellar liposomes of dipalmitoyl-phosphatidylcholine as probed by fluorescence spectroscopy, Photochem. Photobiol. 44 (1986) 151–157.
[10] F. Ricchelli, D. Stevanin, G. Jori, Porphyrin-liposome interactions: influence of the physico-chemical properties of the phospholipid bilayer, Photochem. Photobiol. 48 (1988) 13–18.
[11] F. Ricchelli, S. Gobbo, Porphyrins as fluorescent probes for monitoring phase transition of lipid domains in biological membranes. Factors influencing the microenvironment of haematoporphyrin and protoporphyrin in liposomes, J. Photochem. Photobiol. B. 29 (1995) 65–70.
[12] C. Vever-Bizet, D. Brault, Kinetics of incorporation of porphyrins into small unilamellar vesicles, Biochim. Biophys. Acta. 1153 (1993) 170–174.
[13] A. Lavi, H. Weitman, R.T. Holmes, K.M. Smith, B. Ehrenberg, The depth of porphyrin in a membrane and the membrane's physical properties affect the photosensitizing efficiency, Biophys. J. 82 (2002) 2101–2110.
[14] M. Kepczynski, R.P. Pandian, K.M. Smith, B. Ehrenberg, Do liposome-binding constants of porphyrins correlate with their measured and predicted partitioning between octanol and water? Photochem. Photobiol. 76 (2002) 127–134.
[15] N. Maman, D. Brault, Kinetics of the interactions of a dicarboxylic porphyrin with unilamellar lipidic vesicles: interplay between bilayer thickness and pH in rate control, Biochim. Biophys. Acta 1414 (1998) 31–42.
[16] N.G. Angeli, M.G. Lagorio, E.A. San Roman, L.E. Dicelio, Meso-substituted cationic porphyrins of biological interest. Photophysical and physicochemical properties in solution and bound to liposomes, Photochem. Photobiol. 72 (2000) 49–56.
[17] C. Bombelli, et al., Inclusion of a photosensitizer in liposomes formed by DMPC/gemini surfactant: correlation between physicochemical and biological features of the complexes, J. Med. Chem. 48 (2005) 4882–4891.
[18] H. Mojzisova, S. Bonneau, P. Maillard, K. Berg, D. Brault, Photosensitizing properties of chlorins in solution and in membrane-mimicking systems, J. Photochem. Photobiol. Sci. 8 (2009) 778–787.
[19] I. Voszka, R. Galantai, P. Maillard, G. Csik, Interaction of glycosylated tetraphenyl porphyrins with model lipid membranes of different compositions, J. Photochem. Photobiol. B. 52 (1999) 92–98.
[20] I. Voszka, Z. Szabo, G. Csik, P. Maillard, P. Grof, Interaction of tetraphenylporphyrin derivatives with DPPC-liposomes: an EPR study, J. Photochem. Photobiol. B. 79 (2005) 83–88.
[21] G. Csik, E. Balog, I. Voszka, F. Tolgyesi, D. Oulmi, P. Maillard, M. Momenteau, Glycosylated derivatives of tetraphenyl porphyrin: photophysical characterization, self-aggregation and membrane binding, J. Photochem. Photobiol. B. 44 (1998) 216–224.
[22] R. Bonnett, R.D. White, U.J. Winfield, M.C. Berenbaum, Hydroporphyrins of the meso-tetra(hydroxyphenyl)porphyrin series as tumour photosensitizers, Biochem. J. 261 (1989) 277–280.
[23] I. Laville, S. Pigaglio, J.C. Blais, B. Loock, P. Maillard, D.S. Grierson, J. Blais, A study of the stability of tri(glucosyloxyphenyl)chlorin, a sensitizer for photodynamic therapy, in human colon tumoural cells: a liquid chromatography and MALDI-TOF mass spectrometry analysis, Bioorg. Med. Chem. 12 (2004) 3673–3682.
[24] F. Zsila, Z. Bikadi, M. Simonyi, Unique, pH-dependent biphasic band shape of the visible circular dichroism of curcumin-serum albumin complex, Biochem. Biophys. Res. Commun. 301 (2003) 776–782.
[25] V. Faivre, V. Rosilio, P. Boullanger, L.M. Almeida, A. Baszkin, Fucosyled neoglycolipids: synthesis and interaction with a phospholipid, Chem. Phys. Lipids 109 (2001) 91–101.
[26] L. Schoutteten, P. Denjean, J. Faure, R.B. Pansu, Photophysics of "Calcium Green 1" in vitro and in live cells, Phys. Chem. Chem. Phys. 1 (1999) 2463–2469.

[27] Z.J. Huang, R.P. Haugland, Partition coefficients of fluorescent probes with phospholipid membranes, Biochem. Biophys. Res. Commun. 181 (1991) 166–171.
[28] I. Borissevitch, T.T. Tominaga, H. Imasato, M. Tabak, Fluorescence and optical absorption study of interaction of two water soluble porphyrins with bovine serum albumin. The role of albumin and porphyrin aggregation, J. Lumin. 69 (1996) 65–76.
[29] J. Davilla, A. Harriman, Photochemical and radiolytic oxidation of a zinc porphyrin bound to human serum albumin, J. Am. Chem. Soc. 112 (1990) 2686–2690.
[30] W. Zhang, L. Zhang, G. Ping, Y. Zhang, A. Kettrup, Study on the multiple sites binding of human serum albumin and porphyrin by affinity capillary electrophoresis, J. Chromatogr. B 768 (2002) 211–214.
[31] I. Bardos-Nagy, R. Galantai, A.D. Kaposi, J. Fidy, Difference in the transport of metal and free-base porphyrins - Steady-state and time-resolved fluorescence studies, Int. J. Pharm. 175 (1998) 255–267.
[32] G. Cevc, Phospholipids Handbook, First ed., Technical Univesity of Munich, New York, 1993 (Appendix B).
[33] C.N.H.G. Patonary, I.M. Warner, Bioanalytical applications of fluorescence quenching, Trends Anal. Chem. 5 (1986) 37–43.
[34] L.R. Snyder, J.W. Dolan, Initial experiments in high-performance liquid chromatographic method development. I. Use of a starting gradient run, J. Chromatogr. A 721 (1996) 3–14.
[35] J.D. Krass, B. Jastorff, H.-G. Genieser, Determination of lipophilicity by gradient elution high-performance liquid chromatography, Anal. Chem. 69 (1997) 2575–2585.
[36] W. Humphrey, A. Dalke, K. Schulten, VMD – Visual Molecular Dynamics, J. Mol. Graphics 14 (1996) 33–38, http://www.ks.uiuc.edu/Research/vmd/.
[37] P. Tieleman, Biocomputing at the University of Calgary, Available from: http://moose.bio.ucalgary.ca/.
[38] Molecular Networks, G. Computerchemie, Langemarckplatz 1, Erlangen, Germany. Available from: http://www.molecular-networks.com/.
[39] D. Oulmi, P. Maillard, C. Vever-Bizet, M. Momenteau, D. Brault, Glycosylated porphyrins: characterization of association in aqueous solutions by absorption and fluorescence spectroscopies and determination of singlet oxygen yield in organic media, Photochem. Photobiol. 67 (1998) 511–518.
[40] C.A. Hunter, J.K.M. Sanders, The nature of π–π interactions, J. Am. Chem. Soc. 112 (1990) 5525–5534.
[41] R. Bonnett, Chemical aspects of photodynamic therapy. Advanced chemistry texts, vol. 1, Gordon and Breach Science Publishers, Singapore, 2000, pp. 249–256.
[42] R. Bonnett, B.D. Djelal, A. Nguyen, Physical and chemical studies related to the development of *m*-THPC (FOSCAN) for the photodynamic therapy (PDT) of tumours, J. Porphyrins Phthalocyanines 5 (2001) 652–661.
[43] M. Kasha, H.R. Rawls, M.A. El Bayoumi, The exciton model in molecular spectroscopy, J. Pure Appl. Chem. 11 (1965) 371–392.
[44] C.A. Hunter, J.K.M. Sanders, A.J. Stone, Exciton coupling in porphyrin dimers, J. Chem. Phys. 133 (1989) 395–404.
[45] F. Moro, F.M. Goni, M.A. Urbaneja, Fluorescence quenching at interfaces and the permeation of acrylamide and iodide across phospholipid bilayers, FEBS Lett. 330 (1993) 129–132.
[46] M. Langner, S.W. Hui, Iodide penetration into lipid bilayers as a probe of membrane lipid organization, Chem. Phys. Lipids. 60 (1991) 127–132.
[47] I. Bronshtein, M. Afri, H. Weitman, A.A. Frimer, K.M. Smith, B. Ehrenberg, Porphyrin depth in lipid bilayers as determined by iodide and parallax fluorescence quenching methods and its effect on photosensitizing efficiency, Biophys. J. 87 (2004) 1155–1164.
[48] N.C. Maiti, S. Mazumdar, N. Periasamy, J- and H- aggregates of porphyrin–surfactant complexes: time-resolved fluorescence and other spectroscopic studies, J. Phys. Chem. B 102 (1998) 1528–1538.
[49] J. Zimmermann, U. Siggel, J.-H. Fuhrhop, B. Röder, Excitonic coupling between B and Q transition in a porphyrin aggregate, J. Phys. Chem. B. 107 (2003) 6019–6021.
[50] K.R. Thulborn, W.H. Sawyer, Properties and the locations of a set of fluorescent probes sensitive to the fluidity gradient of the lipid bilayer, Biochim. Biophys. Acta 511 (1978) 125–140.
[51] M. Shinitzky, Y. Barenholz, Fluidity parameters of lipid regions determined by fluorescence polarization, Biochim. Biophys. Acta 515 (1978) 367–394.
[52] M.C. Desroches, A. Kasselouri, M. Meyniel, P. Fontaine, M. Goldmann, P. Prognon, P. Maillard, V. Rosilio, Incorporation of glycoconjugated porphyrin derivatives into phospholipid monolayers: a screening method for the evaluation of their interaction with a cell membrane, Langmuir 20 (2004) 11698–11705.
[53] D.B. Chalpin, A.M. Kleinfeld, Interaction of fluorescence quenchers with the n-(9anthroyloxy) fatty acid membrane probes, Biochim. Biophys. Acta 731 (1983) 465–474.
[54] H.N. Fonda, J.V. Gilbert, R.A. Cormier, J.R. Sprague, K. Kamioka, J.S. Connolly, Spectroscopic, photophysical and redox properties of some meso-substituted free-base porphyrins, J. Phys. Chem. 97 (1993) 7024–7033.
[55] A. Wisniewska, Y. Nishimoto, J.S. Hyde, A. Kusumi, W.K. Subczynski, Depth dependence of the perturbing effect of placing a bulky group (oxazolidine ring spin labels) in the membrane on the membrane phase transition, Biochim. Biophys. Acta 1278 (1996) 68–72.